Performance of Integrated Systems of Automated Roller Shade Systems and Daylight Responsive Dimming Systems

Byoung-Chul Park, Sejong University
An-Seop Choi, Sejong University
Jae-Weon Jeong, Sejong University
Eleanor Lee, Lawrence Berkeley National Laboratory

October 2010

DISCLAIMER

Building and Environment 46 (2011) 747-757

Performance of Integrated Systems: Automated Roller Shade Systems and Daylight Responsive Dimming Systems

Byoung-Chul Park [a], An-Seop Choi [a]*, Jae-Weon Jeong [a], Eleanor S. Lee [b]

[a] *Department of Architectural Engineering, Sejong University, Kunja-Dong, Kwangjin-Gu, Seoul, Korea 143-747*
* *corresponding author e-mail aschoi@sejong.ac.kr fax +82-2-3408-4331*
[b] *Building Technologies Department, Lawrence Berkeley National Laboratory, 1 Cyclotron Road, MS 90R3111 Berkeley, CA 94720*

Abstract

Daylight responsive dimming systems have been used in few buildings to date because they require improvements to improve reliability. The key underlying factor contributing to poor performance is the variability of the ratio of the photosensor signal to daylight workplane illuminance in accordance with sun position, sky condition, and fenestration condition. Therefore, this paper describes the integrated systems between automated roller shade systems and daylight responsive dimming systems with an improved closed-loop proportional control algorithm, and the relative performance of the integrated systems and single systems. The concept of the improved closed-loop proportional control algorithm for the integrated systems is to predict the varying correlation of photosensor signal to daylight workplane illuminance according to roller shade height and sky conditions for improvement of the system accuracy. In this study, the performance of the integrated systems with two improved closed-loop proportional control algorithms was compared with that of the current (modified) closed-loop proportional control algorithm. In the results, the average maintenance percentage and the average discrepancies of the target illuminance, as well as the average time under 90% of target illuminance for the integrated systems significantly improved in comparison with the current closed-loop proportional control algorithm for daylight responsive dimming systems as a single system.

Keywords Integrated systems, automated roller shade systems, daylight responsive dimming systems, daylighting, photoelectric controls.

Nomenclature

$S_T(t)$ = total signal produced by photosensor from daylight and electric light - time-dependent, unit (V)
$S_D(t)$ = daylight component of $S_T(t)$ - time-dependent, unit (V)
$S_E(t)$ = electric light component of $S_T(t)$ - time-dependent, unit (V)
δ = fractional electric lighting output ($\delta_{min} \leq \delta \leq 1$), full output of electric lights $\delta=1$, minimum output of electric lights $\delta=\delta_{min}$
$E_T(t)$ = total light (illuminance) at workplane - time-dependent, unit (lux)
$E_D(t)$ = daylight component of $E_T(t)$ - time-dependent, unit (lux)
$E_E(t)$ = electric light component of $E_T(t)$ - time-dependent, unit (lux)
$S_{1,n}$ = signal produced by photosensor for $\delta=1$ without daylight, unit (V)
$E_{1,n}$ = workplane illuminance level for $\delta=1$ without daylight, unit (lux)
$E_D(t_c)$ = workplane illuminance level by daylight at calibration time, unit (lux)
$S_D(t_c)$ = signal produced by photosensor with daylight at calibration time, unit (V)
M = control slope of the control algorithm, $-M_D/E_{1,n}$, unit (V^{-1})
M_D = correlation of daylight level on the workplane to the photosensor signal, unit (lux/V)
$M_D(t)$ = correlation of daylight level on the workplane to the photosensor signal - time-dependent, unit (lux/V)
$M_D(t_c)$ = correlation of daylight level on the workplane to the photosensor signal at calibration time, unit (lux/V)
K_T = clearness index, the measured global horizontal solar radiation to the calculated extra-terrestrial horizontal radiation
I_d/I = the ratio of diffuse to total irradiance
$C(t)$ = value of the dependent variable (roller shade height or I_d/I ratio in this study)
$C(t_c)$ = value of the dependent variable at calibration time (roller shade height or I_d/I ratio in this study)
R_V = Visible light reflection, the ratio of visible light (380-780 nm) that is reflected from a interior surface
T_V = Visible light transmission, the ratio of visible light (380-780 nm) that is transmitted through a window glass

1. Introduction

Daylight responsive dimming systems have immense potential to significantly reduce energy consumption in buildings, especially high-rise buildings with glass curtain walls. Such systems can save 16–70% of current annual electric lighting consumption, according to past field measurements and simulations [1-4].

Despite their significant technical potential, daylight responsive dimming systems have been used in few buildings to date because they require improvements to improve reliability. The key underlying factor contributing to poor performance (that is, underlit spaces) is the variability of M_D (the ratio of the photosensor signal to daylight workplane illuminance) in accordance with sun position, sky conditions, and fenestration conditions. When the system is commissioned under a given arbitrary sun position, sky condition, and fenestration condition, this M_D in the current control algorithm is set to a fixed value, which results in the design illuminance being undershot under other solar and fenestration conditions.

For daylight responsive dimming systems to be able to capitalize on the available daylight, shading systems are needed to block direct sunlight and introduce available daylight without causing a discomfort glare to occupants. Although M_D varies according to shading system conditions, such as different venetian blind angles and roller shade heights, the current control algorithm uses a fixed M_D at daytime calibration. M_D varies as according to sky conditions as well. Therefore, the variation of M_D with sky and shading system conditions should be considered in designing the control algorithm of daylight responsive dimming systems. Hence, daylight responsive dimming systems should be integrated with automated shading systems to predict varying M_D according to shading system conditions, and the control algorithm for the integrated systems should consider varying M_D with shading system conditions as well as with sky conditions for the system performance.

2. Background

Currently in general use is a modified closed-loop proportional control algorithm based on the conventional closed-loop proportional control algorithm, in which M_D and E_{Em} (maximum electric workplane illuminance), are used to calculate M (control slope) for the determination of dimming level in daylight responsive dimming systems. Although the degradation of E_{Em} was solved using auto-calibration (self-commissioning), varying M_D with sky conditions and fenestration conditions has not been solved.

Auto-calibration of the extent to which degradation of lamps or ballast are degrading is important in achieving system accuracy [5-6]. The artificial lighting illuminance on the workplane at maximum lighting output is generally established at the design level, and the workplane illuminance value with the maximum electric lighting power at night-time calibration is used to determine M in the system control algorithm.

To maintain stable M_D in daylight responsive dimming systems, researchers have established an appropriate photosensor configuration and position [7-12]. Likewise, in order to determine the appropriate M_D at daytime calibration for calculating M in the system algorithm, appropriate calibration times and sky conditions were examined [3-14], and commissioning guidelines presented [1]. Although these studies presented results pertaining to optimum sensor locations, sensor-shielding designs, sensor aiming, and calibration times, the M_D varies according to varying solar and fenestration conditions. Choi and Mistrick (1998) recommended frequent (monthly) commissioning; however, this is difficult in practice because of the costs associated with calibration and the inconvenience caused to working occupants [15].

Direct sunlight is responsible for at least two unwanted effects: (1) discomfort glare to occupants, and (2) increased cooling loads in a space due to the solar and thermal loads from the windows. To block direct sunlight, windows require shading, especially in high-rise buildings with glass curtain walls. Roller shade systems and venetian blinds are popular for this purpose, and automated systems of these kinds are widely used. Automated roller shade systems are generally preferred over venetian blinds in high-rise buildings because the former adjusts easily to produce the appropriate shading conditions. It should also be noted that although venetian blinds must be controlled according to their height and slat angle, roller shade systems can be easily controlled based on height only.

For daylight responsive dimming systems to be able to capitalize on the available daylight, shading systems such as roller shades are needed to block direct sunlight and introduce available daylight without causing a discomfort glare to occupants. To illustrate, the building where *The New York Times* is headquartered has both daylight responsive dimming systems and automated roller shade systems installed [4, 16]; however, the

systems operate separately. Any change to the shading system conditions affects the daylight distribution in a space; thus, the resulting change in the daylight distribution, like the varying M_D in daylight responsive dimming systems, can impair the accuracy of the daylight responsive dimming system. To improve the performance of daylight responsive dimming systems as well as the automated roller shade systems, the two systems should be integrated and provided with an improved control algorithm.

This study hypothesized that two factors affect variation of M_D. The hypothesis is that the variation of M_D is statistically influenced by variations in sky condition and roller shade height (independent variables: sky condition and roller shade heights; dependant variable: M_D), and the varying M_D can be predicted using the independent variable.

To examine the hypothesis for this study, two solstice-to-solstice field experiments were conducted in a full-scale model and a half-scale model of typically daylighted spaces but in different locations, and the data for workplane illuminance, photosensor signals, exterior horizontal irradiance, and roller shaded heights were measured. The first experiment used the full-scale testbed to investigate varying M_D and its trend according to sky condition and roller shade height. The second experiment used the half-scale model in order to provide a basis upon which to validate the results from the first experiment.

The goals of the work described herein are to integrate daylight responsive dimming systems with automated roller shade systems, to present the control algorithm used in this integrated systems, and to compare the integrated system performance to the single system performance. The $M_D(t)$ (time-dependent M_D) was characterized in term of roller shade heights and sky conditions at each of the different roller shade heights. This type of characterization can be integrated into a control algorithm to predict the varying $M_D(t)$, and automated roller shade systems can be integrated with daylight responsive dimming systems as integrated systems. Therefore, integrated systems with a control algorithm were presented and evaluated in this specific case study.

3. Method

3.1 Test facility and conditions

The Windows Testbed Facility with three identical test rooms was located at the Lawrence Berkeley National Laboratory in Berkeley, California (latitude 37°4'N, longitude 122°1'W). Each of the three identical side-by-side furnished test rooms was 3.05 m wide by 4.57 m deep by 3.35 m high and each had a 3.05 m wide by 3.35 m high window wall facing south. A single, interior, top-down roller shade (light-gray basketweave, 3% openness factor) was cycled for 5-minute intervals, each with different roller shade height (6 steps: 0, 0.2, 0.4, 0.6, 0.8, and 1 of roller shade height ratio; the controlled roller shade height to the maximum window height) in a test room. Only the test room data among the three test rooms was used for this study.

Although the system was automatically dimmed during the monitored period for a parallel test objective, the actual lighting system was not significant. The electric lighting value on the workplane was extracted using the derived quadratic fit between power use and electric lighting workplane illuminance from night-time measured data, so that the analysis was only conducted on daylight illuminance. The fit had a 5.13 lux average RMSE (Root Mean Square Error) in a 20-100% dimming range.

The test rooms were monitored over a six-month, solstice-to-solstice period from December 21, 2007, to June 21, 2008. The illuminance, photosensor voltage, and exterior horizontal irradiance data were sampled and recorded at 1-min intervals over a 24 h period using the LabView National Instruments data acquisition software. The test room configuration The six workplane illuminance sensors at 0.76 m facing toward the ceiling were monitored using a color- and cosine-corrected silicone diode photometric sensor (LI-210SA, ±1.5% to 7500 lux, ±0.15% /°C maximum). However, only the average illuminance from the four rear workplane sensors was related to the photosensor signal (Fig. 1); this was because only these sensors were within the photosensor's direct field of view.

The PS-ceil of a shielded photosensor (Perkin Elmer VT5051B, 0.02% /°C) was placed at the south end of the second light fixture, 2.73 m from the window wall and flush with the bottom of the fixture, 2.54 m above the finished floor. The PS-ceil had a 60° cone of view and was pointed downward, normal to the floor. Its view was defined as a circular area on the floor with a radius of 1.47 m.

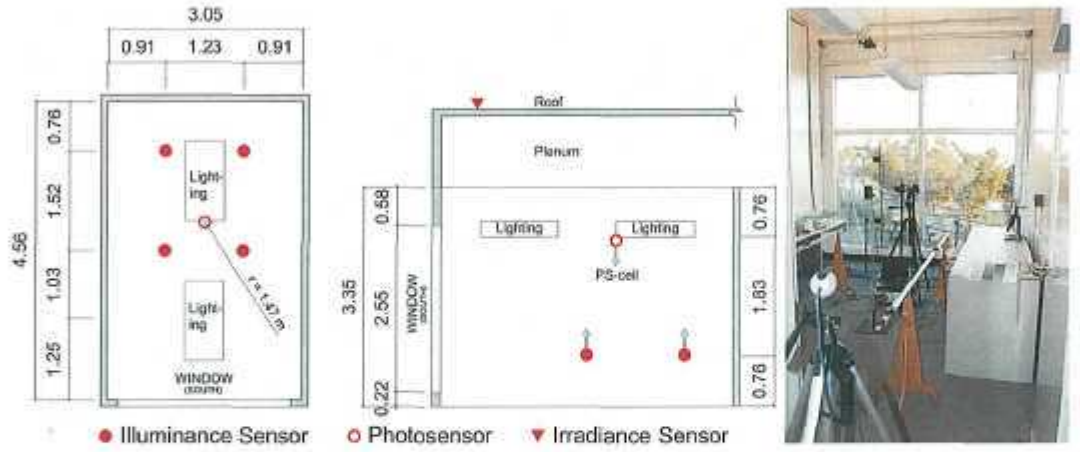

Fig. 1. Floor plan and section for the sensors' positions, and interior view of the test room for the full-scale testbed. Dimensions are given in meters.

An exterior horizontal irradiance sensor (LI-200SA, ±1.0% to 3000W/m^2, ±0.15%/°C) was located on the roof of the testbed. The data was used to calculate K_T (clearness index; the measured global horizontal solar radiation to the calculated extra-terrestrial horizontal radiation) and I_d/I_T (the ratio of diffuse to total irradiance) for classification of sky conditions. A more detailed description of the experimental setup can be found in the study by Lee *et al.* [17].

To verify the trends of the test results in this study, the data were monitored in a half scale mock-up test room at Sejong University, Seoul, Korea (latitude 37°33'N, longitude 127°04'E) (Fig. 2). Each unfurnished test room was 1.51 m wide by 2.87 m deep by 1.57–1.64 m high (inclined roof) and had a 1.22 m wide by 1.29 m high window facing due south. Each room had a single window, which were simultaneously exposed to approximately the same interior and exterior environment. A single, top-down, 3%-open, light-gray (both side) basketweave fiberglass/PVC fabric roller shade was installed in one of the three test rooms. The testbed facility description and roller shade control method in detail are shown in the conference paper by Park and Choi [18].

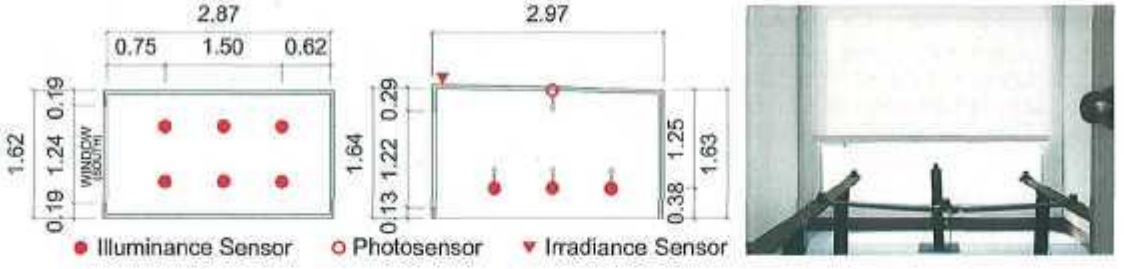

Fig. 2. Floor plan and section for the sensors' positions, and interior view of the test room for the half-scale testbed. Dimensions are given in meters.

3.2 Analysis

Some of the monitored data were eliminated from the datasets used for analysis. Specifically, the following data were eliminated: for 1-min data before and after the roller shade height was changed, the data after sunset within a 10 h period, 8:00 a.m.–18:00 p.m., and the data of the exceeded maximum photosensor signal (>10 V).

The monitored data of cycled roller shade height in the full-scale testbed were analyzed to establish correlations between varying $M_D(t)$ and roller shade heights and sky conditions. I_d/I_T ratio was used as a classification of solar conditions, and this independent variable was used in the analysis of the varying M_D data. The I_d/I_T ratio was calculated using the calculated K_T and I_d/I_T-versus-K_T correlation by Erbs *et al.* (1982), and the K_T values were calculated using the measured global horizontal solar radiation and the calculated extra-terrestrial horizontal radiation [19]. The data for twenty-one days over six-months were analyzed in this study (Table 1).

Table 1
Date of the monitored data used for analysis.

Jan	Feb	Mar	Apr	May	Jun	Sum. of Days
7, 8	7, 8	7-9, 22-24	6, 21-23	10-12, 25-27	10	21

4. Integrated control algorithm with modified closed-loop proportional control algorithm

In this study, the slope of the linear correlation between the photosensor signal and the average daylight workplane illuminance, M_D, was assumed to be adjustable independent variable from the slope of the correlation between the photosensor signal and the average electric lighting workplane illuminance, M_E. With conventional control systems, these two slopes are adjusted simultaneously and are, therefore, interdependent, thereby leading to poor performance. In the study by Lee et al. (1998), the two slopes were set independently and M_D was varied as a function of the venetian blinds' slat angle for an automated prototypical venetian blind–lighting control system [1].

The concept of the modified closed-loop proportional control algorithm is to adjust the electric light level as a linear function of the difference between $S_T(t)$ (total photosensor signal from daylight and electric light) and $S_E(t)$ (electric component of $S_T(t)$) as given by:

$$\delta = M(S_T(t) - S_E(t)) + 1,\ M < 0 \tag{1}$$

The equation of M in the modified closed-loop proportional control algorithm can be derived with $M_D(t_c)$ as in eq. 2, where t_c is the single time of calibration:

$$M(t_c) = \frac{-M_D(t_c)}{E_{lim}} \tag{2}$$

We assumed that if the correlations of the varying $M_D(t)$ to the changed parameters (roller shade height and sky conditions) are directly proportional, $M_D(t)$ can be predicted from at least two daytime calibrations at low and high conditions of the changed parameters. M in the modified closed-loop proportional control algorithm can be continuously adjusted via software as a function of the actual data of roller shade height and a I_d/I_T ratio.

$M_D(t_c)$ can be changed with $M_D(t)$ to predict the varying M_D, and $M_D(t)$ can be modified with Newton's interpolation formula for two calibrations, as shown in eq. 3. It was assumed that the divided conditions of the roller shade height or the I_d/I_T ratio for the two calibrations would be expressed as $C(t_{c1})$ and $C(t_{c2})$:

$$M_D(t) = \frac{M_D(t_{c1}) - M_D(t_{c2})}{C(t_{c1}) - C(t_{c2})}(C(t) - C(t_{c1})) + M_D(t_{c1}) \tag{3}$$

In this study, the performance of the integrated systems, each of which used one of the two improved closed-loop proportional control algorithms using these equations (1-3), one using only the roller shade height and the other using the I_d/I_T ratio at different roller shade heights, was evaluated to compare the modified closed-loop proportional control algorithm in daylight responsive dimming systems as a single system.

5. Results

To illustrate how $M_D(t)$ varies, two parameters — the roller shade height and the I_d/I_T ratio — were tracked on March 22, 2008 (Fig. 3). The varying M_D fluctuated significantly according to the cycled roller shade height, and M_D was also affected by changes in the I_d/I_T ratio.

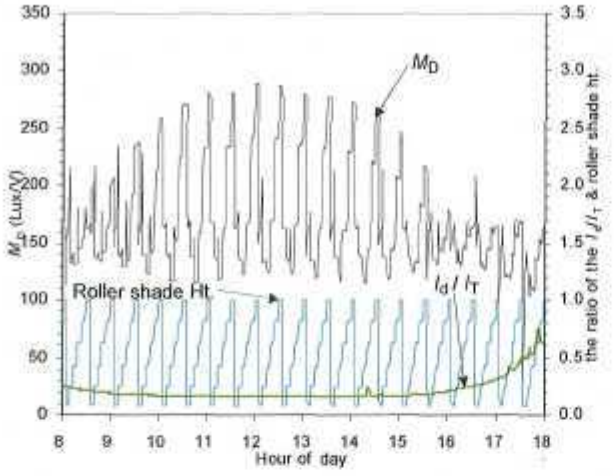

Fig. 3. Trend resulting from varying M_D by roller shade height and I_d/I_T on March 22, 2008.

5.1 M_D vs. roller shade heights

How $M_D(t)$ varies with regard to each roller shade height as a linear relationship using the valid monitored data was examined. The variation of $M_D(t)$ with regard to roller shade height showed that the value of $M_D(t)$ decreased proportionally for a roller shade height ratio form 0 to 0.4, and increased proportionally for a roller shade height ratio form 0.4 to 1. The $M_D(t)$ data to roller shade height for the test period were divided into two ranges, 0–0.4 and 0.4–1.0 ratios of the roller shade height, and derived as two separate linear relationships, where the R^2 values of the correlations were 0.5838 and 0.5770, respectively (Fig. 4). The results indicate that calibrations performed at 0, 0.4, and 1.0 ratios of the roller shade height can be considered. Although 58% reliability is not high, the deviation of the predicted $M_D(t)$ using these correlations will significantly decrease.

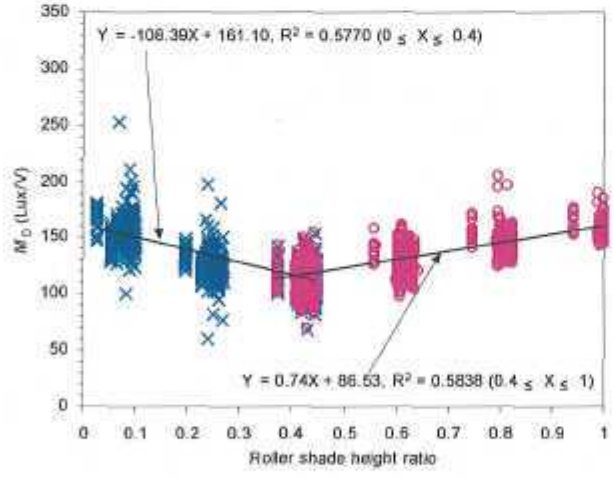

Fig. 4. Linear relationships of M_D to roller shade height in two separate ranges.

5.2 M_D vs. I_d/I_T at the cycled roller shade heights

For each given fixed roller shade height, M_D varies with the I_d/I_T of sky conditions (Fig. 5). The I_d/I_T ($t = 2.17$, $p < 0.05$) at 0.0 of the ratio of the controlled roller shade height to the maximum window height contributed to the varying M_D; however, the R^2 of the linear fit at 0.0 of the ratio of the controlled roller shade height to the maximum window height was also almost zero (R^2=0.0095). So, the I_d/I_T can be ignored at 0.0 of the controlled roller shade height. The R^2 of the linear fit at 0.2, 0.4, 0.6, 0.8, and 1.0 of the ratio of the controlled roller shade height to the maximum roller shade height were 0.2781, 0.6363, 0.4865, 0.3513, and 0.2120 in $p < 0.01$, respectively.

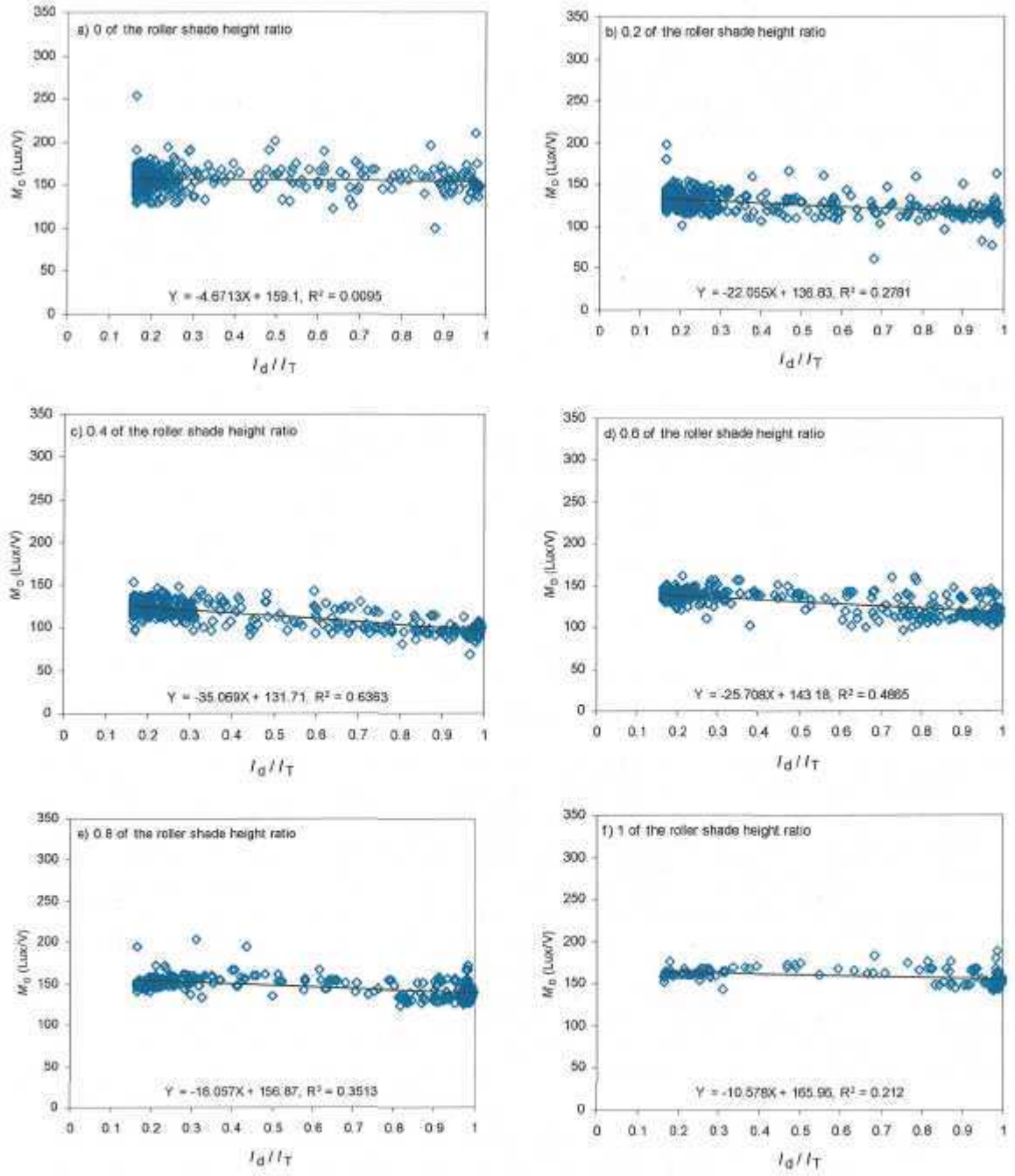

Fig. 5. Linear relationships of M_D to I_d/I_T at different roller shade heights (1=overcast).

When direct sunlight penetrates into a space on the workplane, the roller shade should be down in order to block direct sunlight from the workplane. Therefore, more than 0.6 ratio (60%) of the roller shade height should be used without discomfort glare, such as in the overcast sky condition. Although the roller shade's main function is to block direct sunlight, the automated roller shade system when integrated with a daylight responsive dimming system should be controlled so as to introduce available daylight without discomfort glare.

5.3 Impact of direct sunlight on the correlation of varying $M_D(t)$ to $I_d/I_T(t)$ ratio at each of the cycled roller shade heights

To analyze the effects of direct sunlight on the correlation of varying $M_D(t)$ to the $I_d/I_T(t)$ ratio at each of the cycled roller shade heights, the dataset was classified according to whether direct sunlight interfered or did not interfere with the detection area of the PS-ceil on the floor. A sun profile angle was used to calculate the penetration distance to the PS-ceil detection area.

The total data and two divided data were compared based on a linear relationship of $M_D(t)$ to $I_d/I_T(t)$ (Table 2). The R^2 of the derived fit of $M_D(t)$ to $I_d/I_T(t)$ was increased with a small gap when the interfering data to the PS-ceil detection area were excluded. Occupants tend to close roller shades when direct sunlight interferes with their desks or when discomfort glare occurs. Therefore, to render reliable the linear relationship of $M_D(t)$ to $I_d/I_T(t)$ in the improved closed-loop proportional control systems, direct sunlight must be blocked without a perimeter zone, and the roller shade height should be controlled without interference by direct sunlight in the detection area of the photosensor.

Table 2
Linear relationship of M_D to I_d/I_T at different roller shade heights as expressed by the divided data with and without interference of the PS-ceil detecting area.

Data condition		Statistics	Ratio of roller shade height (controlled height/maximum height)					
			0	0.2	0.4	0.6	0.8	1
PS-ceil	Total data	Slope	-4.67	-22.05	-35.07	-25.71	-18.06	-10.58
		R2	0.0095	0.2781	0.6363	0.4865	0.3513	0.2120
		RMSE	12.66	9.53	8.14	8.61	8.52	7.17
	Un-interfered data	Slope	-4.67	-22.18	-36.49	-28.64	-18.58	-11.18
		R2	0.0095	0.2818	0.6747	0.6250	0.4685	0.3795
		RMSE	12.66	9.30	7.58	6.88	6.71	5.34
	Interfered data	Slope	-	-6.64	-37.59	-27.65	-24.30	-13.19
		R2	-	0.0233	0.5624	0.3205	0.3991	0.2080
		RMSE	-	12.34	10.26	12.51	9.98	7.97

5.4 Performance of the integrated systems with each improved closed-loop proportional control algorithm

The performance of the integrated systems each of which used one of the two improved closed-loop proportional control algorithms - one using only roller shade height and the other using the I_d/I_i ratio at different roller shade heights — was evaluated to compare the modified closed-loop proportional control algorithm in daylight responsive dimming systems as a single system. Firstly, only the roller shade height as an independent variable for predicting varying M_D was integrated into the improved closed-loop proportional control algorithm for the integrated systems. In this case, the I_d/I_T ratio was ignored for the simple system with no added component for the integrated systems. To consider the I_d/I_T ratio for the integrated systems, a horizontal global exterior irradiance sensor should be used to calculate the I_d/I_T ratio, and this added component increases the initial costs. Secondly, the I_d/I_T ratio at different roller shade heights as an independent variable for predicting varying M_D was integrated into the improved closed-loop proportional control algorithm to improve system accuracy. Although the second improved closed-loop proportional control system could be further improved by diverse and frequent calibrations, the initial cost of doing so would increase because the latter would entail measuring the exterior global irradiance on the horizontal surface.

The integrated systems, each of which used one of the improved closed-loop proportional control algorithms, were compared with the daylight responsive dimming systems, which used the current closed-loop proportional control algorithm (modified closed-loop proportional control algorithm) using monitored data for the 8:00 a.m.–18:00 p.m. period over 21 days. The integrated systems were separated based on two conditions: roller shade height and the I_d/I_T ratio at different roller shade heights. The electric component of the workplane illuminance was calculated from the δ determined by M_D in each control algorithm, and added to the measured daylight component in order to derive the total workplane illuminance.

To calculate M for the current daylight responsive dimming systems, a single daytime-calibration is generally performed when the sky condition is not partly cloudy and there is no direct sunlight in the room [1]. In this study, multi-calibration was adopted to calculate M for the two integrated systems. For the integrated systems with the improved closed-loop proportional control algorithm using only the roller shade height, three calibrations at 0, 0.4, and 1 of the ratio of the controlled roller shaded height to its maximum for each linear relationship 0–0.4 and 0.4–1 of the ratio were adopted. For the integrated systems, with the improved closed-

loop proportional control algorithm using the I_d/I_T ratio at different roller shade heights, a single calibration at 0 of the roller shade height ratio was adopted, and each of the two calibrations at 0.2, 0.4, 0.6, 0.8, and 1.0 of the ratio was adopted. Each of the roller shade heights for the calibrations was a representative value for each of the roller shade height range. Each calibration dataset was collected at around 15:00 PM on April 21 and 22, 2008, and the conditions and conditional expressions are shown in Table 3.

Table 3
Conditions at calibrations for each of the control algorithms and the derived functions of M and δ.

Control Algorithm	Conditions at Calibration			M	Transfer Function
	Height ratio	I_d/I_T	M_{ic}		
Modified closed-loop proportional	0	0.19	155.76	$M = -0.29$	$\delta = M(S_T(t)-S_i(t)) + 1$
Improved closed-loop proportional - Roller shade height	0	0.19	155.76	$M(t_{ic}) = (69.46C(t_{ic})-155.76)/543,\ 0 \le Ht \le 0.4$	$\delta = M(t_{ic})(S_T(t)-S_i(t)) + 1$
	0.4	0.20	127.97		
				$M(t_{ic}) = (-58.66C(t_{ic})+104.51)/543,\ 0.4 < Ht \le 1$	
	1	0.21	163.17		
Improved closed-loop proportional - I_d/I_T at different roller shade height	0	0.19	155.76	$M(t_{ic}) = (69.46C(t_{ic})-155.76)/543,\ 0 \le Ht \le 0.1$	$\delta = M(t_{ic})(S_T(t)-S_i(t)) + 1$
	0.2	0.20	141.02	$M(t_{ic}) = (-1.99C(t_{ic})+140.62)/543,\ 0.1 < Ht \le 0.3$	
		0.77	142.15		
	0.4	0.20	127.97	$M(t_{ic}) = (40.38C(t_{ic})+136.21)/543,\ 0.3 < Ht \le 0.5$	
		0.95	97.89		
	0.6	0.21	138.92	$M(t_{ic}) = (25.27C(t_{ic})+144.18)/543,\ 0.5 < Ht \le 0.7$	
		0.97	119.55		
	0.8	0.21	152.91	$M(t_{ic}) = (8.86C(t_{ic})+154.81)/543,\ 0.7 < Ht \le 0.9$	
		0.98	146.17		
	1	0.22	163.17	$M(t_{ic}) = (6.53C(t_{ic})+164.58)/543,\ 0.9 < Ht \le 1.0$	
		0.98	158.18		

The performance of each of the system algorithms was evaluated and then compared using the monitored data (Table 4). The integrated systems with either of the improved closed-loop proportional control algorithms achieved a system performance that was more accurate than that of the single system with the modified closed-loop proportional control algorithm. The average maintenance percentages of the target illuminance for the single daylight responsive dimming systems, the integrated systems using only roller shade height, and the

integrated systems using the I_d/I_T ratio at different roller shade heights were around 97.1, 98.2, and 98.7%, respectively, and their average discrepancies were 40.23 (±42.40) lux, 28.59 (±36.86) lux, and 24.94 (±37.07) lux, respectively. The values of the standard deviation on the derived average discrepancies were larger than the average values. The discrepancies were highly skewed when roller shade height changed (e.g. especially from 0.4 to 0.6 ratio of roller shade height). Although the average maintenance percentages did not increase significantly, the average discrepancies and the average error time (min) under 90% of target illuminance per day as an inadequate value decreased significantly in the both integrated systems.

Table 4
Comparison of the control algorithms based on the average difference between the predicted and measured workplane illuminance, the maintenance percentage of target illuminance, and the average time under 90% of target illuminance throughout a day (8:00–18:00).

Items	Modified closed-loop proportional		Improved closed-loop proportional with roller shade Ht		Improved closed-loop proportional with I_d/I_T at different roller shade ht	
	Mean	St Dev	Mean	St Dev	Mean	St Dev
Difference (lux)	40 23	42 40	28 59	36 86	24 94	37 07
Maintenance (%)	97 09	7 25	98 22	5 73	98 71	5 13
Under 90% target illuminance (min/day)	66 33	53 21	24 71	30 35	12 95	12 76

5.5 Cause of inadequate M in each improved closed-loop proportional control algorithm

Insufficient data under 90% of the target illuminance were collected to examine causes of inadequate workplane illuminance in the integrated systems with the improved closed-loop proportional control algorithm. The data were analyzed based on roller shade height, I_d/I_T ratio, solar position, and penetration of the photosensor detecting area. The day with the most errors in each month was selected as the basis on which to determine the causes of errors (Fig. 6).

Interference by direct sunlight in the PS-cell detecting area was not the main cause of the errors; only 16.5% of total errors in one integrated system and 10.4% in the other were affected by direct sunlight (data not shown). There were some patterns of high-frequency for roller shade height, I_d/I_T ratio, and solar position, with both integrated systems showing similar results (Fig. 6). Except for the June 10 data, the frequency was high at around a 0.4 ratio (40%) of the controlled roller shade height to its maximum height and the I_d/I_T ratio was also high. The errors in the integrated systems using only roller shade height primarily occurred under -45° and over 45° of azimuth with low altitude in January, February, and March; the errors, however, occurred widely at from -90° to 90° of azimuth after March. However, the errors in the integrated systems using the I_d/I_T ratio at different roller shade heights decreased significantly between -45° and 45° of azimuth after March.

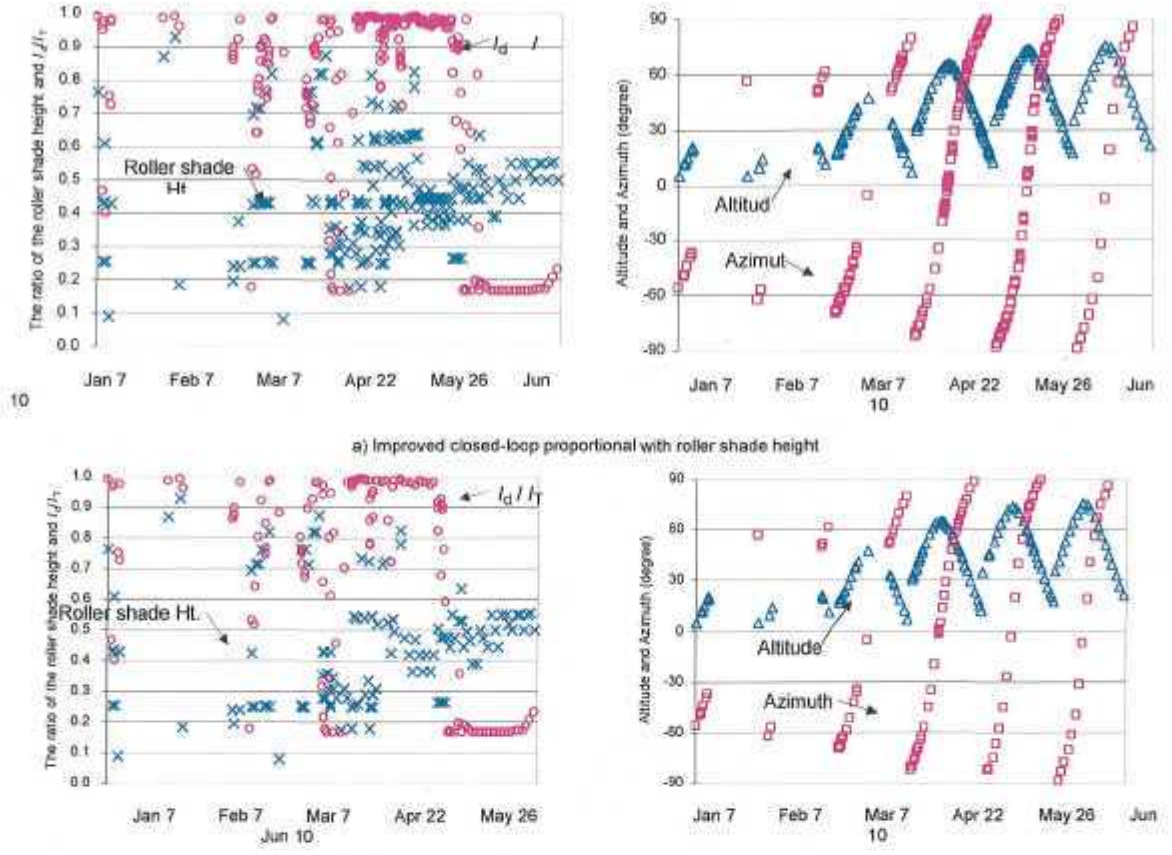

Fig. 6. Distribution of errors based on I_d/I_T ratio, roller shade height, and solar positions.

5.6 Verification of the results using extra test

To compare the full-scale testbed and the half-scale testbed results, the fifteen-day data collected during the solstice-to-solstice test period were included in the dataset for analysis. In the dataset, the controlled roller shade height was varied from 0 to around 0.3 of the ratio (the controlled roller shade height to its maximum height) throughout the course of a day. This condition can be compared with the result from the full-scale testbed in Fig. 4, which is a correlation of varying M_D to roller shade height under 0.4 of the roller shade height ratio.

To examine whether the correlation of the varying M_D to roller shade height is different, the correlation of $M_D(t)$ to the controlled roller shade height from the data monitored in the half-scale testbed was derived and given in Fig. 7, such as in Fig. 4. Unlike the results from the full-scale testbed, this M_D trend gradually increased. The dataset was divided based on 0.13 of the roller shade height, as (1) the trend of the varying M_D to the increased roller shade height at 0–0.13 of roller shade height is flat, and then (2) the trend of 0.13–0.32 gradually increased. This seems to be the turning point, as 0.4 of the roller shade height (Fig. 4) occurred at around 0.1 of the roller shade height.

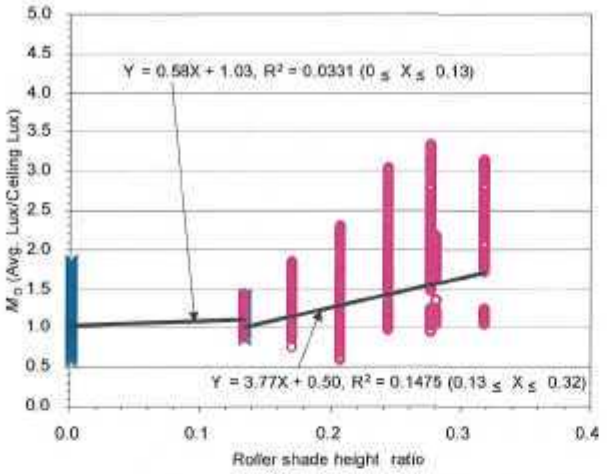

Fig. 7. Linear relationship of M_D to roller shade height in half-scale mock-up.

To examine how different photosensor location and configuration affect the trend of varying M_D to roller shade height, computer simulations using RADIANCE 3.8 for Linux were conducted based on the same location and different photosensor conditions. The simulation results were compared to the results of the full-scale testbed and half-scale testbed.

The conditions of test room size, interior surface reflectances, window transmittance, 60° photosensor, and shade material were identical to those of the full-scale testbed. And, the conditions of the full-scale testbed location and the 180° photosensor were identical to those of the half-scale testbed. The simulation conditions are shown in Table 5 and Fig. 8. For reference, the computed R_V and T_V for this RADIANCE simulation were calculated using their RGB reflectance or transmittance.

Table 5
Test room conditions on the location, size, roller shade, interior surface reflectance, and window transmittance for computer simulation.

Location	Latitude 37°33'N, longitude 127°04'E, Seoul
Test room size	3.05 m wide by 4.57 m deep by 3.35 m high
Roller shade	3% openness factor, 6-step roller shade height for 0.2 interval
Interior surface reflectance (R_V)	Ceiling (0.86), wall (0.85), floor (0.18)
Window transmittance (T_V)	0.62

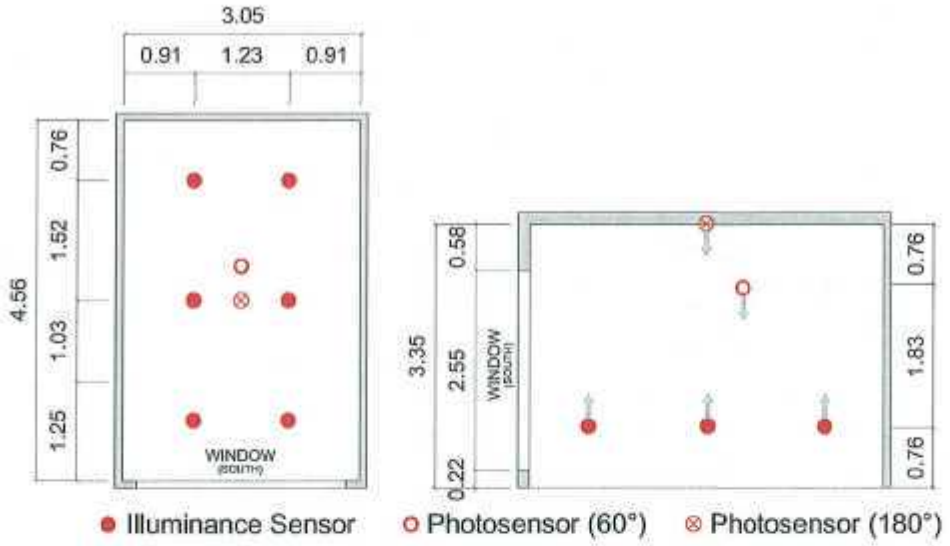

Fig. 8. Calculation point on the photosensor signal and workplane illuminance. Dimensions are given in meters.

Conducted with a variety of roller shade heights under diverse sky conditions (+s, -s, -i, and -c for "Gensky" of RADIANCE 3.8 for Linux), the hourly computer simulations took place 9:00 a.m.–18:00 p.m. on Dec 21, Mar 21, and Jun 21. Firstly, the trend of the varying M_D to roller shade height under the various sky conditions on the 180° photosensor located in the middle of the ceiling surface was derived, as shown in Fig. 9. Secondly, the trend on the 60° photosensor located 2.54 m above the finished floor was derived, as shown in Fig. 10.

Fig. 9 shows that the turning point occurred at 0.1 of the roller shade height. This result can be compared with the results of Fig. 7 for the half-scale testbed, which shows that the full-scale and half-scale testbeds evinced a similar turning point with regard to the correlation of M_D to roller shade height.

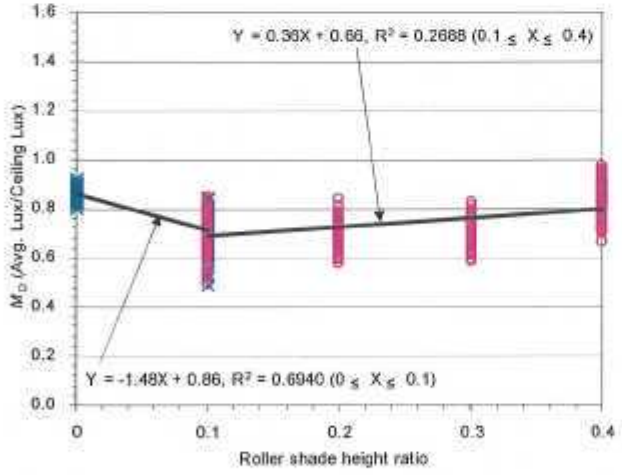

Fig. 9. Linear relationship of M_D to roller shade height on the 180° photosensor.

The trend of the 60° photosensor (Fig. 10) shows that the lowest value in correlating M_D to roller shade height occurred at 0.3 of the roller shade height. This result can be compared with those for the full-scale testbed (Fig. 4): the full-scale and half-scale testbeds showed a similar turning point in correlating M_D to roller shade height.

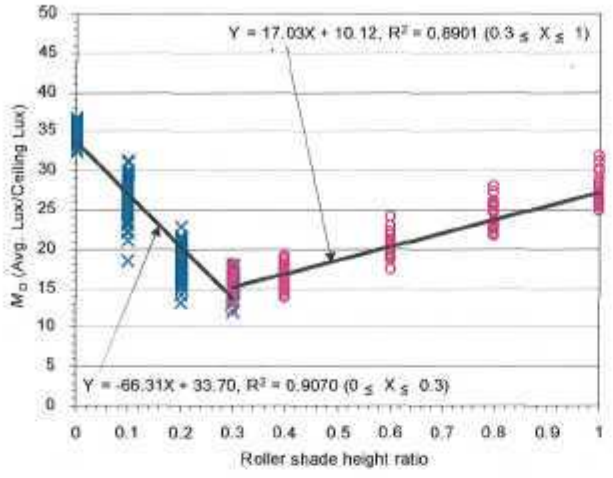

Fig. 10. Linear relationship of M_D to roller shade height on the 60° photosensor.

Therefore, the correlation of M_D to roller shade height shows a trend expressed as a "V" line. To use the improved control algorithm for the integrated systems, the correlation of the varying M_D to roller shade height should be separated in two ranges in order to achieve a linear relationship. The turning point, critical for dividing the two roller shade height ranges, is significantly affected by both the configuration and the position of the photosensor.

6. Discussion

When valid M_D data were separated at a 0.4 ratio of the roller shade height, the varying $M_D(t)$ was shown as having a linear relationship. The roller shade height was cycled at 0.2 ratio intervals of the controlled height to maximum height. The 0.4 ratio of the roller shade height as a turning point from the results of full-scale testbed could be changed more or less than 0.4 ratio when the roller shade was cycled at intervals of less than a 0.2 ratio of the roller shade height.

The reliability of PS-ceil is decreased when direct sunlight interfered in the PS-ceil detecting area. The reliability of the derived linear fit of I_d/I_T to the varying M_D on the PS-ceil improved when the interfered data were excluded. Therefore, to improve the accuracy of the integrated systems, which can control roller shade height for available daylight in a space as well as artificial lighting output for energy savings, direct sunlight into the photosensor-detecting area should be blocked using roller shade system for the reliability of PS-ceil. The photosensor detecting area should be determined with the permitted distance of direct sunlight from window, such as 1.25 m in Fig. 3, because the direct sunlight can lead discomfort glare as well as electric lighting energy savings.

The performance of the integrated systems with the two improved closed-loop proportional control algorithms was evaluated. This performance was compared with that of the daylight responsive dimming systems with the modified closed-loop proportional control algorithm, that is, the algorithm that is currently in general use. Although the modified closed-loop proportional control algorithm uses the fixed M, the improved closed-loop proportional control algorithm uses the changed M to respond to varying roller shade heights and I_d/I_T ratios. The performance comparison showed that the average maintenance percent to the target illuminance for both the improved closed-loop proportional control algorithms was slightly higher than that of the modified closed-loop proportional control algorithm, but the average error time under 90% of the target illuminance significantly decreased for the former. As in actual applications, the minimum number of calibrations was assumed to evaluate the performance of the improved closed-loop proportional control algorithm. It can be assumed that the more sophisticated calibration (more than two calibrations) in each subdivided condition is likely to achieve further performance improvements.

Inadequate workplane illuminance errors in the improved closed-loop proportional control algorithm occurred frequently when the sun leaned to the east and west on the plane; these errors also occurred frequently when the I_d/I_T ratio was high. It can be assumed that if direct sunlight were controlled in the azimuth so as to be redirected

through a window into a space less than 45° (absolute value) of the sun's azimuth angle using an exterior shading system, such as a vertical shade, then the number of errors would decrease.

To validate the result from full-scale testbed, the dataset monitored in the half-scale testbed was analyzed based on the correlation of M_D to the roller shade height. In this analysis, the turning point of 0.4 roller shade height ratio in Fig. 4 shifted toward a lower roller shade height of around 0.1 roller shade height ratio. The computer simulation results validated the correlation trend of the M_D to the roller shade height for the full- and half-scale testbeds. It was found that the photosensor configuration and position affect the turning point level of the correlation of the M_D to the roller shade height. Therefore, the improved control algorithm for the integrated systems can be adopted in a space with automated roller shade systems and daylight responsive dimming systems.

7. Conclusions

The fixed M_D to calculate M is used in current control algorithm of daylight responsive dimming systems, and this causes inadequate workplane illuminance due to the variation of M_D across a day. To render the performance of daylight responsive dimming system more accurate, a field-test was conducted for this study.

To integrate automated roller shade systems and daylight responsive dimming systems, the effects of roller shade height and I_d/I_T ratio on M_D were investigated using the data obtained from the test room with cycled roller shade heights (6 steps for a 5-min interval). Varying M_D was adopted into the control algorithm for integrated systems when the former was directly proportional to independent variables such as roller shade height and I_d/I_T ratio at each different roller shade height.

The integrated system performance was relatively compared to the single system performance in this study. To compare the two improved closed-loop proportional control algorithms for the integrated systems and the current closed-loop control algorithm for daylight responsive dimming systems as a single system, three monitored data, the average maintenance percentage, the average discrepancies, and the average time under 90% based on the target illuminance, were calculated and compared for each algorithm. Both improved closed-loop proportional control algorithms for each of the integrated systems were significantly improved when compared to the current closed-loop proportional control algorithm.

To improve the performance accuracy of daylight responsive dimming systems, information regarding roller shade height should be included in the control software for the improvement of the closed-loop proportional control algorithm. Through an integration of software of daylight responsive dimming systems and automated roller shade systems, the improved closed-loop proportional control algorithm could be used in conventional daylight responsive dimming systems with no added components. However, also needed are integrated systems with the improved closed-loop proportional control algorithm using the I_d/I_T ratio for different roller shade heights that would include an additional component. That is, an exterior global irradiance sensor is required to calculate the I_d/I_T ratio. Although the addition of an irradiance sensor to this integrated system means that the initial costs are higher, the system accuracy is significantly improved based on this study. Therefore, the improved system accuracy could be instrumental in accelerating market adoption of daylight responsive dimming systems.

Acknowledgments

We would like to acknowledge and thank R.D Clear for statistical data extraction. We would like also to acknowledge and thank R.D Clear, S.E. Selkowitz, D.L. DiBartolomeo and K. Konis for their contributions to the field test at the Windows Testbed Facility, Lawrence Berkeley National Laboratory.

This work was also supported by Samsung Corporation, by the Assistant Secretary for Energy Efficiency and Renewable Energy, Office of Building Technology, State and Community Programs, Office of Building Research and Standards of the U.S. Department of Energy under Contract No. DE-AC02-05CH11231, and by the California Energy Commission through its Public Interest Energy Research (PIER) Program. And, the main author was funded by 2nd Brain Korea 21 project.

References

[1] Lee, E.S., DiBartolomeo, D.L., Selkowitz, S.E., 1998. The Effect of Venetian Blinds on Daylight Photoelectric Control Performance. Journal of the Illuminating Engineering Society 28, 3-23.

[2] Rubinstein, F., Jennings, J., Avery, D., Blanc, S., 1999. Preliminary Results from an Advanced Lighting Controls Testbed. Journal of the Illuminating Engineering Society 28, 130-141.

[3] Choi, A., Sung, M., 2000. Development of a Daylight Responsive Dimming System and Preliminary Evaluation of System Performance. Building and Environment 35, 663-676.

[4] Lee, E.S., Selkowitz, S.E., 2006. The New York Times Headquarters Daylighting Mockup: Monitored Performance of the Daylighting Control System. Energy and Buildings 38, 914-929.

[5] Roche, L., 2002. Summertime Performance of an Automated Lighting and Blinds Control System. Lighting Research and Technology 34, 11-27.

[6] Koyle, B., Papamichael, K., Pistochini, T., 2009. Improved Daylighting Controls through Dual Loop Sensing. Oral session presented at the IESNA Annual Conference Seattle, WA.

[7] Mistrick, R.G., Chen, C., Bierman, A., Felts, D., 2000. A Comparison of Photosensor-Controlled Electronic Dimming Systems in a Small Office. Journal of the Illuminating Engineering Society 28, 59-73.

[8] Rubinstein, F., 1984. Photoelectric Control of Equi-Illumination Lighting Systems. Energy and Buildings 6, 141-150.

[9] Rubinstein, F., Ward, G., Verderber, R., 1989. Improving the Performance of Photoelectrically Controlled Lighting Systems. Journal of the Illuminating Engineering Society 18, 70-94.

[10] Ranasinghe, S., Mistrick, R.G., 2003. A Study of Photosensor Configuration and Performance in a Dyalighted Classroom Space. Journal of the Illuminating Engineering Society 32, 3-20.

[11] Choi, A., Song, K., Kim, Y., 2005. The Characteristics of Photosensors and Electronic Dimming Ballasts in Daylight Responsive Dimming Systems. Building and Environment 40, 39-50.

[12] Kim, S., Kim, J., 2007. The Impact of Daylight Fluctuation on a Daylight Dimming Control System in a Small Office. Energy and Buildings 39, 935-944.

[13] Choi, A., Mistrick, R.G., 1997. On the Prediction of Energy Savings for a Daylight Dimming System. Journal of the Illuminating Engineering Society 26, 77-90.

[14] Kim, S., Mistrick, R.G., 2001. Recommended Daylight Conditions for Photosensor System Calibration in a Small Office. Journal of the Illuminating Engineering Society 30, 176-188.

[15] Choi, A., Mistrick, R.G., 1998. Analysis of Daylight Responsive Dimming System Performance. Building and Environment 34, 231-243.

[16] NYSERDA, 2005. Daylighting the New York Times Headquarters Building. Final Report 06-05, 16.

[17] Lee, E.S., DiBartolomeo, D.L., Klems, J.H., Konis, K., Clear, R.D., Yazdanian, M., et al., 2009. Field measurements of innovative indoor shading systems in a full-scale office testbed. ASHRAE transactions 115.

[18] Park, B., Choi, A., 2009. A Study on the Improvement of Accuracy of Daylight Responsive Dimming Systems' Algorithm. 2nd China, Japan, and Korea Lighting Symposium Sapporo.

[19] Erbs, D.G., Klein, S.A., Duffie, J.A., 1982. Estimation of the Diffuse Radiation Fraction for Hourly, Daily and Monthly-Average Global Radiation. Solar Energy 28, 293-302.